Available online at www.sciencedirect.com
SCIENCE DIRECT
Polymer 46 (2005) 10364–10371
polymer
www.elsevier.com/locate/polymer

The effect of moisture on the dynamical mechanical properties of bacterial cellulose/glucuronoxylan nanocomposites

Sofia Dammström[a], Lennart Salmén[b], Paul Gatenholm[a,*]

[a]*Department of Chemical and Biological Engineering, Biopolymer Technology, Chalmers University of Technology, Kemivägen 10, SE-412 96 Göteborg, Sweden*
[b]*STFI-Packforsk AB, Box 5604, SE-114 86 Stockholm, Sweden*

Received 4 July 2005; received in revised form 20 July 2005; accepted 29 July 2005
Available online 25 August 2005

Abstract

The plant cell wall possesses unique material properties due to its hierarchical organisation. In order to biomimic a native structure like a plant cell wall, a model system consisting of microfibrillar cellulose, produced by the gram-negative bacteria *Acetobacter xylinum*, and a glucuronoxylan matrix derived from aspen holocellulose was constructed. The glucuronoxylan was extracted from delignified aspen (*Populus tremula*) wood chips using DMSO to preserve its native chemical composition. Dynamic mechanical analysis (DMA) measurements performed with moisture scans showed a moisture-induced softening of delignified aspen wood fibres due to the plasticization of glucuronoxylan. A similar result was observed for the model system. However, the softening behaviour of the delignified aspen fibre and the model system was not identical, most probably due to differences in spatial organisation of the components. Dynamic FTIR-studies indicated that interactions between the cellulose and the glucuronoxylan exist in the aspen holocellulose while the components in the nanocomposite appear to be more isolated.

Keywords: Nanocomposites; Glucuronoxylan; Material properties

1. Introduction

There is a growing interest in the utilisation of biological materials, such as wood, not only as construction materials or as a raw material for pulp and paper production, but also as a new feedstock for the development of advanced biocomposites with tailor-made properties. Therefore, wood is an excellent source of inspiration for the design of a new generation high-performance material.

The plants have developed a way of combining different building blocks into a hierarchical structure and thereby obtain unique properties such as stiffness, low density and toughness, resulting in wood being an extraordinary composite material. The main structural framework of all plant cell walls is formed by cellulosic- and non-cellulosic-polysaccharides together with pectins and aromatic compounds. However, the molecular composition of the cell wall polymers varies among species, tissues etc. [1]. Although the wood cell wall is the most abundant construction element on earth, the precise structural arrangement and the interfacial interactions between its constituents are far from fully understood. However, the composition of the cell wall has been thoroughly investigated and there is a profound knowledge about structure and appearance of the individual components, presented in several comprehensive reviews [2–9].

Early models of the wood cell wall described its construction as a composition of individual and interacting layers of cellulose, polysaccharide matrix and lignin [10,11]. At later stages the models developed towards a more intimate distribution of the constituents. The structure was described as bundles of cellulose microfibrils embedded in a matrix of amorphous non-cellulosic polysaccharides and lignin [12,13]. Following these studies a number of even more sophisticated models have been proposed and several reviews have been published [14–16]. Regarding the interactions and interplay between the wood cell wall components it has been suggested that the non-cellulosic

* Corresponding author. Tel.: +46 31 7723407; fax: +46 31 7723418.
E-mail address: paul.gatenholm@chem.chalmers.se (P. Gatenholm).

0032-3861/$ - see front matter © 2005 Elsevier Ltd. All rights reserved.
doi:10.1016/j.polymer.2005.07.105

polysaccharides, hereafter referred to as hemicelluloses, play an important role in the aggregation pattern of the cellulose microfibrils by affecting the crystalline structure and changing the dimensions of the cellulose microfibrils [17–21]. In addition to the change in cellulose conformation it has been suggested that the hemicelluloses also influence the structure of the lignin during cell wall biosynthesis [19]. It has been proposed that the hierarchical organisation of the cell wall of higher plants starts at the nanoscale level and that the secondary and tertiary levels of the molecular structure of the constituents are coupled [19].

The material properties of wood and other biological materials are strongly influenced by moisture content, whereas synthetic materials are significantly affected by temperature changes. When increasing the temperature, a majority of the synthetic polymers undergo secondary transitions and then melt. In contrast, most biological materials are being degraded before any glass transition appears and they do not show any melting behaviour. However, since water can act as a plasticizer for many biopolymers [22] it is possible to observe the glass transition of the material by studying the effect of moisture on the material properties. To study these effects in spruce fibres, Salmén and Olsson [23] used dynamic mechanical analysis (DMA) with a moisture scan instead of a temperature scan. The study was performed on delignified spruce fibres with preserved native structural arrangement of cellulose and hemicelluloses and also on spruce pulp fibres. The main structural elements of spruce fibres are cellulose, lignin and the hemicelluloses glucuronoxylan and glucomannan [1]. Based on the difference in softening behaviour as an effect of changes in the relative surrounding humidity (RH), it was concluded that a distinct structural difference between glucuronoxylan and glucomannan probably occurs within the spruce fibre wall. The glucuronoxylan appeared to be associated with the lignin while the glucomannan appeared to be more tightly associated to the cellulose, a fact confirmed by dynamic FTIR studies [24]. Dynamic FTIR has been proven to be a useful tool in studying the molecular polymer–polymer interactions in wood fibres [24–27] and can be used to study the influence of moisture on the softening of wood polymers [28].

To further study the interfacial interactions between cellulose and glucuronoxylan in the plant cell wall a biomimetic model based on bacterial cellulose and *O*-acetyl-(4-*O*-methylglucurono)xylan isolated from aspen (*Populus tremula*) was developed [29]. This new model provides a useful tool for the design of future 'wood-inspired' materials based on renewable resources. The great advantage in using bacterial cellulose as a model for plant cellulose lies in its high purity and fine fibrils. A disadvantage, however, is the high crystallinity. The glucuronoxylan used for this model has been isolated by dimethylsulfoxide extraction of aspen wood chips, a procedure that preserves the native acetylated structure. The aim of this study was to address the effect of moisture on the interfacial interaction between cellulose microfibrils and glucuronoxylan in the biomimetic model. To verify whether the nanocomposite structure can be related to the native wood cell wall, delignified aspen fibres with maintained structural arrangement of cellulose and glucuronoxylan has been used as a reference.

2. Experimental

2.1. Materials

2.1.1. Bacterial cellulose

The cellulose was produced by static cultivation of *Acetobacter xylinum*, sub species BPR2001, in a fructose/CSL medium at 30 °C [30]. The bacteria were grown in 400 mL erlenmeyer flasks containing 100 mL of media. In order to remove the bacteria and to exchange remaining media, the produced cellulose pellicles were boiled in 1 M NaOH at 80 °C for 1 h followed by repetitive boiling in deionised water. To prevent drying and to avoid contamination, the washed cellulose was stored in diluted ethanol in a refrigerator.

2.1.2. Aspen holocellulose

Aspen wood chips were ground and dried in a vacuum oven at 50 °C over night. Twenty grams dry meal was placed in a three-necked round bottom flask. Fifty millilitre of 1.33 M sodium chlorite, 50 mL of 1.66 M sodium acetate and 2 mL of concentrated acetic acid were mixed together and the total volume was adjusted to 400 mL with deionised water (70 °C) before addition to the aspen meal. The mixture was left under magnetic stirring and temperature control at 70 ° C for 30 min before another addition of 50 mL sodium chlorite and 2 mL acetic acid. Sodium chlorite and acetic acid were then added every 24 h during 6 days [31,32]. Remaining chlorine gas was removed by flushing nitrogen gas through the flask for 3 h. The slurry was cooled to 4 ° C and the solids were filtered off on a Büchner funnel covered with a fine nylon mesh. The resulting solid material consists of delignified fibres, which are referred to as holocellulose. The holocellulose was washed with 3 L of deionised water (50 °C) before it was dried in a vacuum oven at 50 °C over night. The resulting dry weight was 12 g, which was 60% of the initial dry weight. The relative composition of the holocellulose is presented in Table 1.

Table 1
Composition of the aspen holocellulose (w/w)

Glucuronoxylan	10.4%
Galactoglucomannan	2.5%
Cellulose	85.1%
Lignin (Klason)	~1%

2.1.3. Glucuronoxylan

The glucuronoxylan used in this work was an *O*-acetyl-(4-*O*-methylglucurono)xylan prepared by DMSO extraction of the aspen holocellulose. Extraction was made with a holocellulose:DMSO ratio of 1:20 at 60 °C for 24 h and the remaining filtrate was freeze dried.

The carbohydrate composition of the resulting DMSO-extracted glucuronoxylan is presented in Table 2. The glucuronoxylan had a molecular weight of 10,530 g/mol and $DS_{Acetyl} = 0.52$ (based on the glucuronoxylan chain, possible substitutions of the side group sugars are not considered). In its native state glucuronoxylan has been reported to have $DS_{Acetyl} = 0.6–0.7$ [2].

2.1.4. Bacterial cellulose/glucuronoxylan nanocomposites and glucuronoxylan film

Cellulose pellicles were homogenised in water by use of a Waring Laboratory blender LB20E. The speed schedule followed was: 1 min at speed level 6, 2 min at speed level 8 and 2 min at speed level 12. Homogenisation was performed at room temperature and resulted in a microfibril suspension. The glucuronoxylan was dissolved in water and heated under stirring at 95 °C for 15 min. The glucuronoxylan was then added to the microfibril suspension and the blend was left under stirring for 30 min at room temperature. The resulting gel was distributed among three polystyrene petri-dishes, 14 cm diameter, and dried at 23 °C, 50% relative humidity. The film containing only glucuronoxylan was prepared from a pure glucuronoxylan solution heated at 95° for 15 min, poured into a polystyrene petri-dish and dried at the same conditions as the composite films.

2.2. Methods

2.2.1. Atomic force microscopy

A small piece of the sample was mounted on magnetic holders using adhesive tabs to keep the sample in position during the analysis. The instrument used was a Digital Instrument (Santa Barbara, USA) Dimension 3000 with a G-type scanner and a standard silicon tip. The frequency used was 317 kHz and the analysis was performed in tapping mode with moderate tapping. An area of the sample measuring $2 \times 2\ \mu m^2$ was scanned.

2.2.2. Scanning electron microscopy

SEM-pictures were taken at different magnifications with a Zeiss DSM 940 scanning electron microscope. In order to obtain a conducting material the samples were sputtered with gold before analysis.

Table 2
Relative carbohydrate composition of the DMSO extracted glucuronoxylan

Xylose	92.72%
Glucose	3.14%
Mannose	2.14%
Rhamnose	0.57%
Cellobiose	0.43%

All percent values are weight of monomers based on starting material.

2.2.3. Dynamical mechanical testing

The mechanical testing was performed using a Perkin–Elmer DMA 7. Measurements were performed in humidity scans at a temperature of 30 ° C. The amplitude was set to be constant at 5 μm and the static load equal to 120% of the dynamic load. The frequency used was 1 Hz. Humidity scans were created by a computer-controlled humidifier, which produces humid air by mixing dry, and fully saturated air streams. After initial conditioning at 30% RH for 15 min, a ramp from 30 to 90% RH was set with 1% RH/min. The airflow was 1.4 l/min. The relative modulus and the phase angle were studied in order to characterise the softening behaviour of the sample.

2.2.4. Dynamic vapour sorption

The moisture content in the samples was determined at different relative humidities by use of a Surface Measurement Systems Plus II Oven DVS. Starting at 0% RH, the humidity was kept constant for 500 min before raising the level 10% units stepwise to a final humidity of 90%. Total gas flow was 0.2 L/s. The weight increase of the sample was recorded as a function of the change in humidity of the surrounding air.

2.2.5. Dynamic FTIR

Spectra were recorded on a FTS 6000 FTIR spectrometer (Digilab, Randolph, MA, USA). The collector used was a liquid nitrogen cooled MCT (Mercury Cadmium Telluride) detector and the transmission spectra were recorded with a resolution of $8\ cm^{-1}$. Samples of size 22×30 mm were placed in the holders and a pre-load of ~30% of the stress at break was applied before conditioning for 1 h. During collection of the FT-IR spectra a sinusoidal strain (<0.3%) was applied to the sample with a frequency of 16 Hz. The interferometer was run in step-scan mode with a scanning speed of 0.5 Hz and a phase modulation of 400 Hz. Four scans were co-added. The resulting interferrograms were Fourier transformed and digital signal processing extracted the dynamic changes in the transmission spectrum of the sample from the detector signal. The resulting spectra were normalised to 1.0 at the $1430\ cm^{-1}$ band corresponding to the cellulose.

3. Results and discussion

3.1. Morphology

Scanning electron microscopy (SEM) has been used to study the morphology of the films (Fig. 1). The films of bacterial cellulose, BC, had a sandwich-like, laminar structure consisting of a completely random network of

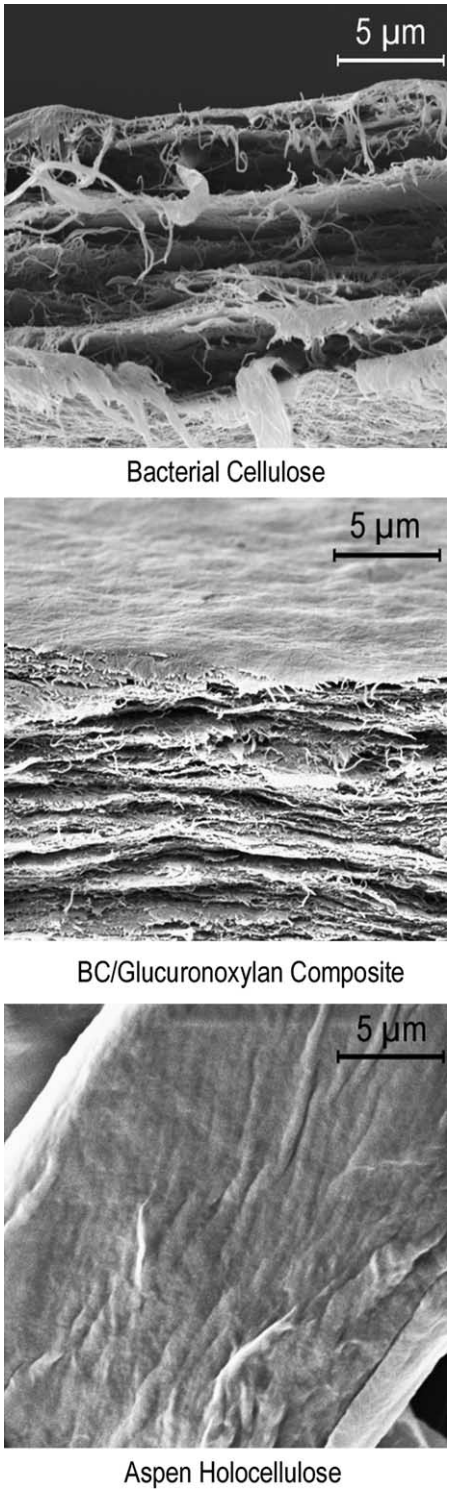

Fig. 1. SEM pictures of films taken with 5000× magnification.

cellulose microfibrils. It appears as if the structure became denser when glucuronoxylan was present (middle).

Atomic force microscopy (AFM) was also used for the morphology studies. The phase image of the reference sample of bacterial cellulose showed microfibrils arranged in bundles with a diameter of approximately 60–100 nm (Fig. 2, top). In the composite, the bundles were covered

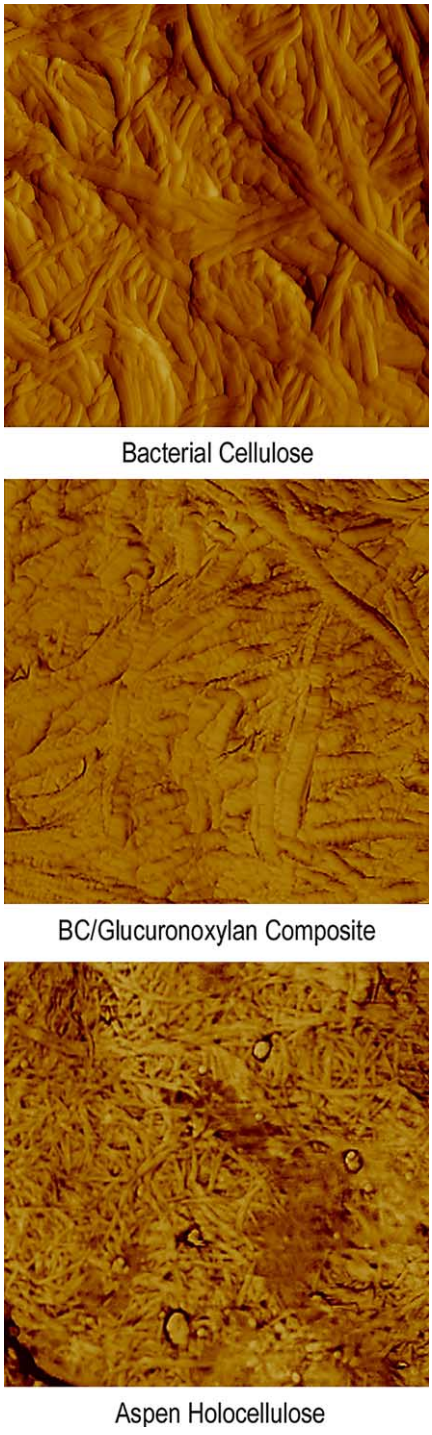

Fig. 2. AFM pictures of an area $2\times2\ \mu m^2$ of the samples. Top: Bacterial cellulose, phase image, z-range = 45.8 de. Middle: BC/glucuronoxylan composite, phase image, z-range = 46.5 de. Bottom: Aspen holocellulose, phase image, z-range = 31.8 de.

with an evenly distributed layer of glucuronoxylan (Fig. 2, middle). On the contrary, the microfibrils in the aspen holocellulose sample (Fig. 2, bottom) had a thinner diameter and cavities between the microfibrils were visible. These cavities result probably from the removal of lignin and/or lignin/polysaccharide matrix. However, it was not possible

to see any glucuronoxylan layer on each microfibril. One possible reason for the difference in appearance is the spatial distribution of the cellulose and glucuronoxylan, which is a consequence of different assembly processes. During cell wall assembly the glucuronoxylan may get in contact with the cellulose during the cellulose aggregation process. This possibly results in a more intimate contact between cellulose and glucuronoxylan. Each cellulose microfibril that is visible with AFM may in fact be a nano-organised hierarchical structure of cellulose and glucuronoxylan.

3.2. Dynamic mechanical analysis

Fig. 3 shows humidity scans at 1 Hz, 30 °C, for films made of pure bacterial cellulose (top left), pure glucuronoxylan (top right), a mixture of 50% bacterial cellulose + 50% glucuronoxylan (bottom left) and aspen holocellulose (bottom right). No softening was detectable for the reference sample of pure bacterial cellulose while a pronounced decrease in modulus at about 85% RH was detected for the pure aspen glucuronoxylan. The composite film made from bacterial cellulose with aspen glucuronoxylan as a matrix also showed a prominent decrease in modulus but at a slightly lower surrounding relative humidity as compared to the pure glucuronoxylan. Since no softening appeared for the pure bacterial cellulose one may conclude that the softening of the bacterial cellulose/glucuronoxylan composite was caused by a moisture-induced glass transition of the glucuronoxylan. However, the presence of cellulose microfibrils has an impact on the softening behaviour, resulting in a less steep decline of the curve. The softening of the holocellulose appeared at approximately the same humidity as for the composite. Here too it is reasonable to presume that the softening was due to the plasticization caused by the glass transition of the glucuronoxylan. In addition, however, it is likely that some of the softening was due to the plasticization of moisture sensitive parts of the wood fibre cellulose fibrils, as shown for spruce [22]. The appearance of the modulus decrease for the holocellulose sample also reminds of a cross-linked polymer system. One may speculate that the presence of molecular interactions between cellulose and glucuronoxylan might restrict the moisture-induced mobility of the glucuronoxylan chains.

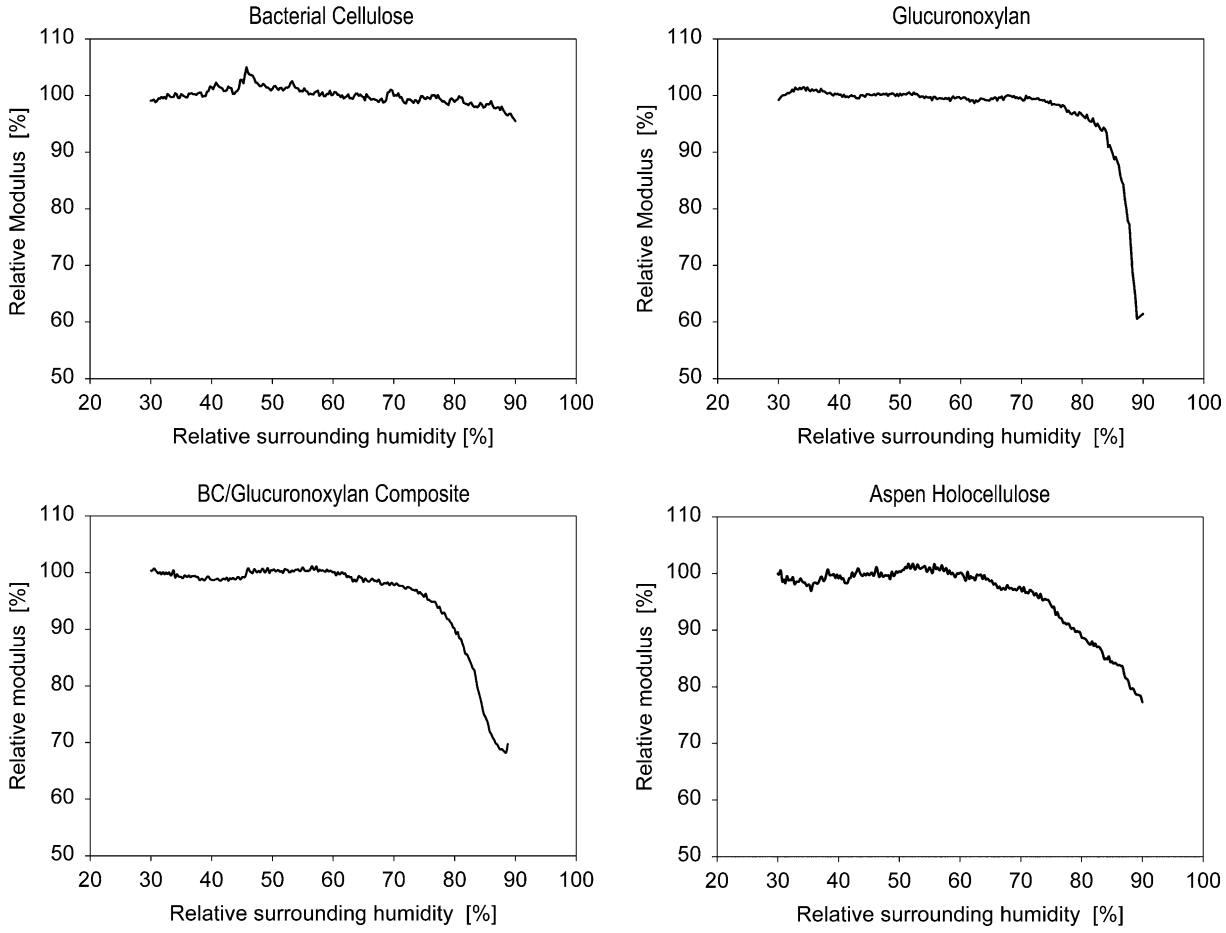

Fig. 3. The decrease in modulus as an effect of an increased relative humidity for films containing pure bacterial cellulose (top left), pure glucuronoxylan (top right), bacterial cellulose/glucuronoxylan nanocomposite (bottom left) and aspen holocellulose (bottom right).

3.3. Moisture content

It has been previously shown [33] that the amount of adsorbed water decreases with an increased degree of acetylation and that a glucuronoxylan with $DS_{Ac}=0.6$ adsorbs approximately 21% water at 90% RH. The glucuronoxylan used in this work had a $DS_{Ac}\approx0.52$ and it was found to contain 24.7% water at 90% RH (Fig. 4). The bacterial cellulose/glucuronoxylan composite film contained 16.4% water, the holocellulose contained 14.3% and the pure bacterial cellulose contained 12.7% moisture at 90% RH (Fig. 4). The water molecules are adsorbed around polar groups in the amorphous regions of the cellulose [34,35], which implies that the low water uptake of the bacterial cellulose is in agreement with its relatively high crystallinity (approximately 70% [36]). It is notable that the difference in moisture uptake between the composite film, the holocellulose and the pure bacterial cellulose is surprisingly small. It is also notable that the obtained value for the holocellulose is somewhat low in comparison to what would be expected for such a pulp [37], which might be related to the relatively low hemicellulose content in this sample.

3.4. Dynamic FTIR

When the sample is slightly stretched, the molecules will respond in different ways depending on their local surroundings. The dipole-transitions will change direction, change conformation or stay unaffected. Only those groups that are affected by the stretching will be seen as a change in spectral intensity and unaffected groups will not give any absorption bands at all in dynamic FTIR. Either a positive or a negative absorption band will result if the molecular vibration changes direction as a result of the IR radiation being polarised. Split absorption bands, i.e. one positive and one negative band directly after each other, appears if a chemical bond changes its vibrational energy. The direct response of molecular groups corresponds to the elastic component of the sample and is given as the in-phase signal of the spectrum. The time-delayed responses result in the out-of-phase signal, representing the viscous component of the sample. [24]

The dynamic FTIR-spectrum for the aspen holocellulose recorded at 30 °C, 0° polarisation and at a relative humidity of 0% is seen in Fig. 5(top). There were strong elastic signals at the wave-numbers 1430 and 1319 cm^{-1}, typically assigned to the cellulose molecule. According to literature the signal at $\sim$1315 cm^{-1} came from wagging (out of the plane) of the CH_2-groups and the signal at 1430 cm^{-1} originated from CH_2-scissoring [38,39]. However, later work stated that the signal at 1430 cm^{-1} more likely derived from C–O–H bending [25]. Either way, the signal originated from the cellulose molecule.

There were also strong elastic signals at the wave-numbers 1735 and 1257 cm^{-1}. The signal at 1735 cm^{-1} were assigned to the C=O bond of the acetyl group on the glucuronoxylan and the 1257 cm^{-1} signal came from the R–O link in the acetyl group on the glucuronoxylan [40]. Dynamic FTIR spectroscopy solely shows intensity changes as a result of straining and only those polymers that are

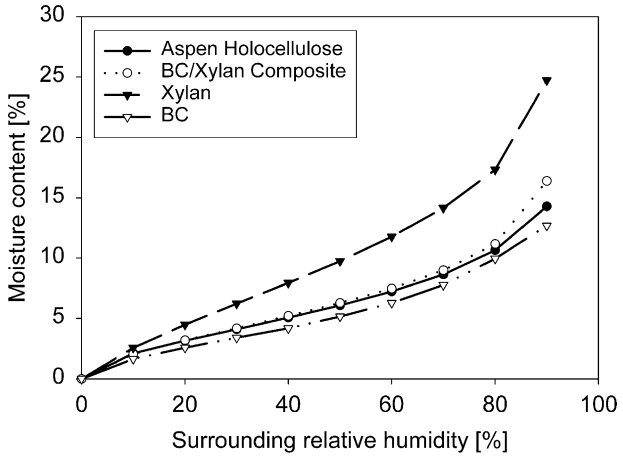

Fig. 4. Moisture content as a function of surrounding relative humidity.

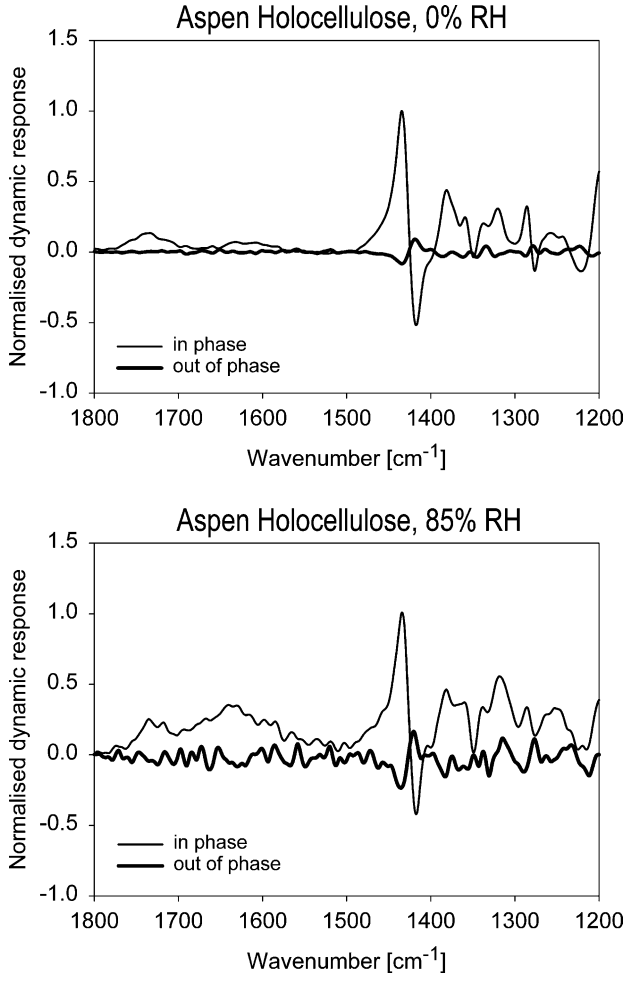

Fig. 5. Dynamic FTIR-spectrum of aspen holocellulose. Top: Recorded at 0% surrounding relative humidity, 30 °C, 0° polarisation. Bottom: Recorded at 85% surrounding relative humidity, 30 °C, 0° polarisation.

involved in the stress transfer will contribute to the dynamic spectrum. Since there were strong elastic signals from both the cellulose and the glucuronoxylan it can be concluded that both these polymers participate in the load transfer and it is reasonable to believe that there are some sort of interactions between the components. When the spectrum was recorded at 85% RH (Fig. 5, bottom) a broad elastic signal appeared at 1630 cm^{-1}. Both adsorbed water and the carboxylate ion of glucuronoxylan have high absorptivity in this region and this signal may reflect either a change in water content or a change in the physical state of glucuronoxylan. Since the DMA measurements showed a softening of the material at 85% RH a physical change is probable and one could therefore assume an increase of the viscous signal in the dynamic IR-spectra. Although there was a general increase of the out-of-phase, viscous signal at 85% RH no wave number specific signals were seen. This indicates that there are interactions between the cellulose microfibrils and the glucuronoxylan and that these interactions hinder the expected viscous behaviour of the glucuronoxylan. However, since the glucuronoxylan content of the used holocellulose is relatively low (~10%) it might also be an effect of the glucuronoxylan amount being too small in order to make its viscous influence detectable.

The spectra for the composite recorded under dry conditions (Fig. 6, top) looked quite similar to the one recorded for the aspen holocellulose. The bacterial cellulose/glucuronoxylan nanocomposite also showed strong elastic signals from the cellulose at wave-numbers 1430 and 1319 cm^{-1} and from the glucuronoxylan at 1735 and 1257 cm^{-1}. The signal at 1257 cm^{-1} was especially strong, a matter that remains unexplained. When the humidity was increased to 85% RH (Fig. 6, bottom) there was a pronounced viscous signal from the glucuronoxylan. This means that there are no interactions between the glucuronoxylan and the cellulose that hinders the viscous behaviour of the glucuronoxylan. Conclusively one can speculate that the glucuronoxylan is present in sufficiently large amounts in order to participate in the stress transfer but no clear indication for cellulose–xylan interactions could be observed.

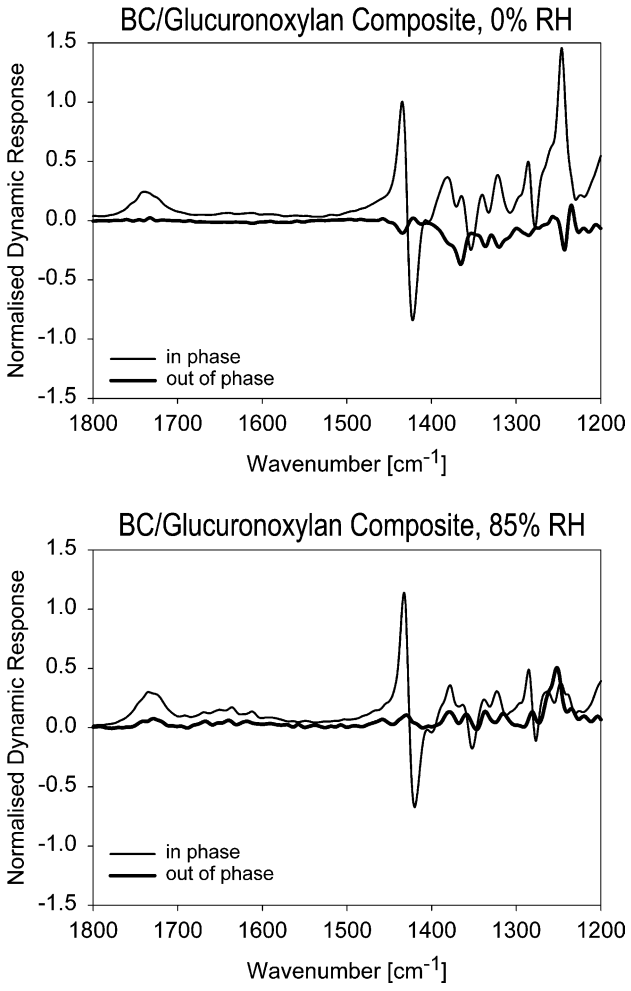

Fig. 6. Dynamic FTIR-spectrum of the composite. Top: Recorded at 0% surrounding relative humidity, 30 °C, 0° polarisation. Bottom: Recorded at 85% surrounding relative humidity, 30 °C, 0° polarisation.

4. Conclusions

Based on the results from DMA-measurements it was concluded that the moisture induced softening of delignified aspen wood fibres was due to the interactions between glucuronoxylan and water and the resulting plasticization. The same observations could be made for the nanocomposite based on bacterial cellulose and aspen glucuronoxylan. However, the softening behaviour of the delignified aspen fibre and the nanocomposite was not identical, most probably due to differences in spatial organisation of the components. By use of dynamic FTIR-studies it was confirmed that there were interactions between the cellulose and the glucuronoxylan in the delignified aspen fibres. Since earlier studies [23,24] performed on birch and spruce fibres showed very weak interactions between the cellulose and glucuronoxylan and stronger interactions between cellulose and glucomannan it was likely to believe that the organisation of the polymers could be species specific and may vary depending on the type of wood that was studied. No clear interactions could be observed between the glucuronoxylan and the cellulose in the composite. Possible explanations are the relatively large amount of matrix glucuronoxylan or poor contact between the glucuronoxylan phase and the cellulose microfibrils. An attempt to achieve better contact between the two components by optimization of the blending ratios is currently being evaluated in our laboratories.

Acknowledgements

The Bo Rydin Foundation for Scientific Research is gratefully acknowledged for financial support. The authors

also wish to express their gratitude to Margaretha Åkerholm and Jasna Stevanic-Srndovic at STFI-Packforsk for carrying out the dynamic FTIR-measurements and to Anne-Mari Olsson at STFI-Packforsk for invaluable help with the DMA and DVS measurements. Johannes Roubroeks is also acknowledged for valuable comments and review of the manuscript.

References

[1] Sjostrom E. Wood chemistry, fundamentals and applications. London, UK: Academic Press; 1983.
[2] Timell TE. Wood Sci Technol 1967;1:45–70.
[3] Atalla RH. In: Pinto BM, editor. Celluloses. Comprehensive natural products chemistry, vol. 3. Amsterdam, The Netherlands: Elsevier Science B.V.; 1999. p. 529–98.
[4] Atalla RH. ACS Symp Ser 1987;340:1–14.
[5] Atalla RH, Hackney JM. Mater Res Soc Symp Proc 1992;255:387–97.
[6] Brown Jr RM. J Macromol Sci, Pure Appl Chem 1996;A33(10): 1345–73.
[7] Brown Jr RM. J Polym Sci, Part A: Polym Chem 2004;42(3):487–95.
[8] Brown Jr RM, Saxena IM. Plant Physiol Biochem 2000;38(1/2): 57–67.
[9] Delmer DP, Stone BA. In: Preiss J, editor. Biosynthesis of plant cell walls. Biochem Plants, vol. 14. San Diego, CA: Academic; 1988. p. 373–420.
[10] Fengel D. Tappi 1970;53(3):497–503.
[11] Kerr AJ, Goring DAI. Cell Chem Technol 1975;9:563–73.
[12] Page DH. Wood Fiber 1976;7:246–8.
[13] Terashima N, Fukushima K, He L-F, Takabe K. In: Jung HG, Buxton DR, Hatfield RD, Ralph J, editors. Comprehensive model of the lignified plant cell wall. Forage cell wall structure and digestibility. Madison, WI: ASA-CSSA-SSSA; 1993. p. 247–70.
[14] Carpita NC, Gibeaut DM. Plant J 1993;3(1):1–30.
[15] Carpita NC, McCann M. In: Buchanan B, Gruissem W, Jones R, editors. The cell wall. Biochemistry and molecular biology of plants. Rockville, MD, USA: American Society of Plant Physiologists; 2000. p. 52–108.
[16] Fujita M, Harada H. In: Hon DN-S, Shiraishi N, editors. Ultrastructure and formation of wood cell wall. 2nd ed. Wood and cellulosic chemistry, 2nd ed. New York, NY: Marcel Dekker; 2001. p. 1–49.
[17] Hackney JM, Atalla RH, VanderHart DL. Int J Biol Macromol 1994; 16(4):215–8.
[18] Uhlin KI, Atalla RH, Thompson NS. Cellulose 1995;2(2):129–44.
[19] Terashima N, Atalla RH. Formation and structure of lignified plant cell wall—factors controlling lignin structure during its formation. In: International symposium on wood and pulping chemistry, 8th, Helsinki, June 6–9, 1995; 1: 69–76.
[20] Iwata T, Indrarti L, Azuma J-I. Cellulose 1998;5(3):215–28.
[21] Tokoh C, Takabe K, Sugiyama J, Fujita M. Cellulose 2002;9(1): 65–74.
[22] Levine H, Slade L. In: Franks F, editor. Water as plasticizer: Physico-chemical aspects of low moisture polymeric systems. Water science reviews. Cambridge, UK: Cambridge University press; 1988. p. 79–185.
[23] Salmén L, Olsson AM. J Pulp Pap Sci 1998;24(3):99–103.
[24] Akerholm M, Salmén L. Polymer 2001;42(3):963–9.
[25] Hinterstoisser B, Akerholm M, Salmén L. Carbohydr Res 2001; 334(1):27–37.
[26] Akerholm M, Salmén L. Holzforschung 2003;57(5):459–65.
[27] Akerolm M, Salmén L. J Pulp Pap Sci 2002;28(7):245–9.
[28] Akerholm M, Hinterstoisser B, Salmén L. Carbohydr Res 2004; 339(3):569–78.
[29] Dammstrom S, Gatenholm P. In: Stokke D, Groom LH, editors. Preparation and properties of cellulose/xylan nanocomposites. Characterization of the cellulosic cell wall. Ames, Iowa USA: Blackwell Publishing; 2005, chapter 5.
[30] Matsuoka M, Tsuchida T, Matsushita K, Adachi O, Yoshinaga F. Biosci Biotechnol Biochem 1996;60(4):575–9.
[31] Wise LE, Murphy M, D'Addieco AA. Pap Trade J 1946;122(2): 35–43.
[32] Timell TE. Tappi 1961;44:88–96.
[33] Grondahl M, Teleman A, Gatenholm P. Carbohydr Polym 2003;52: 359–66.
[34] Valentine L. J Polym Sci 1958;27:313.
[35] Nakamura K, Hatakeyama T, Hatakeyama H. Text Res 1981;51:607.
[36] Yoshinaga F, Tonuchi N, Watanabe K. Biosci Biotechnol Biochem 1997;61(2):219–24.
[37] Berthold J, Rinaudo M, Salmén L. Colloid Surf 1996;112:117–29.
[38] Liang CY, Marchessault RH. J Polym Sci 1959;39:269–78.
[39] Nelsson ML, O'Connor RT. J Appl Polym Sci 1964;8:1325–41.
[40] Marchessault RH. Pure Appl Chem 1962;5:107–29.